Formation of Periodic Nanostructures on Aluminum Surface by Femtosecond Laser Pulses

E. V. Golosov[a], A. A. Ionin[b], Yu. R. Kolobov[a], S. I. Kudryashov[b], A. E. Ligachev[c], S. V. Makarov[b, d], Yu. N. Novoselov[b], L. V. Seleznev[b], and D. V. Sinitsyn[b]

[a] *Belgorod State University, Belgorod, 308015 Russia*
[b] *Lebedev Physical Institute, Russian Academy of Sciences, Moscow, 119991 Russia*
[c] *Prokhorov Institute of General Physics, Russian Academy of Sciences, Moscow, 119991 Russia*
[d] *Moscow Engineering Physics Institute, National Research Nuclear University, Moscow, 115409 Russia*

Abstract—One-dimensional periodic nanostructures have been produced on the surface of an aluminum specimen using femtosecond laser pulses at wavelengths of 744 and 248 nm. The nanostructurization of the specimen has been conducted in water and in air in the preablation regime. We investigate the dependence that the surface topology has on the parameters of laser radiation (wavelength, fluence, and number of pulses), as well as on the medium in contact with the specimen surface. A calculation of the optical characteristics of aluminum as they depend on the electron temperature is performed that is good at describing the dependence that the reflection of the *p*-polarized infrared femtosecond pulses of pumping has on the fluence. Using these optical characteristics of the photoexcited aluminum within the interferential model, periods of the aluminum surface nanogratings are estimated which are in good agreement with the periods measured experimentally.

INTRODUCTION

As is known, the properties of nanostructurized surfaces of metals are essentially different from their volume properties, which is the basis for nonlinear optical effects like surface-enhanced Raman scattering and the second-harmonic generation [1, 2]. Periodic structures with micron dimensions obtained by traditionally focusing powerful laser radiation on the metal surface were first demonstrated experimentally more than 40 years ago [3]. Since then, such structures, as well as structures with a period well below a wavelength, have been repeatedly obtained on the surfaces of metals [4, 5] and semiconductors [6, 7]. However, for aluminum, which is one of the most fundamental materials for modern microelectronics and an advanced material for nanophotonics and nanoplasmonics, the results obtained earlier are very contradictory; completely different types of nanostructures formed on the surface in [8] and in [9] under similar experimental conditions.

In this work, one-dimensional periodic nanostructures are imprinted on a mechanically polished aluminum surface under the action of femtosecond laser pulses with different surface fluences, which are then investigated using a scanning electron microscope (SEM) with a magnification reaching 100 000. The nanostructure periods measured experimentally show a good agreement with the periods calculated within the interferential model [10] for different values of fluence of the incident laser radiation with the use of the calculated optical characteristics of the photoexcited material.

EXPERIMENTAL

In our experiments we used the linearly polarized radiation of the basic harmonic (the central wavelength $\lambda \approx 744$ nm; FWHM parameter of 12 nm) and of the third harmonic (the central wavelength $\lambda \approx 248$ nm; FWHM parameter of 1.5 nm) of the femtosecond Ti:sapphire laser setup (Fig. 1) with a duration of infrared (IR) and ultraviolet (UV) pulses of about 100 fs (in the interaction area), an energy reaching 8 mJ [4] (for the third harmonic it reached 0.5 mJ), and a repetition rate of 10 Hz; the lateral spatial distribution of the laser field corresponded to the TEM_{00} mode. The energy of laser pulses was controlled and checked using the reflection polarization attenuators for the appropriate spectral range (Avesta Project) and the calibration photodiode DET-210 (Thorlab) illuminated by weak laser glare via the rotating dielectric mirror. The energy value of the laser radiation (<0.8 mJ) is selected so that the noticeable degradation of the fluence distribution over the target surface, which is connected to self-focusing in air and the combined effects of chromatic emission, filamentation, and scattering in plasma, should be avoided.

The imprinting of nanostructural spots (individual points and tracks) was done by focusing laser radiation

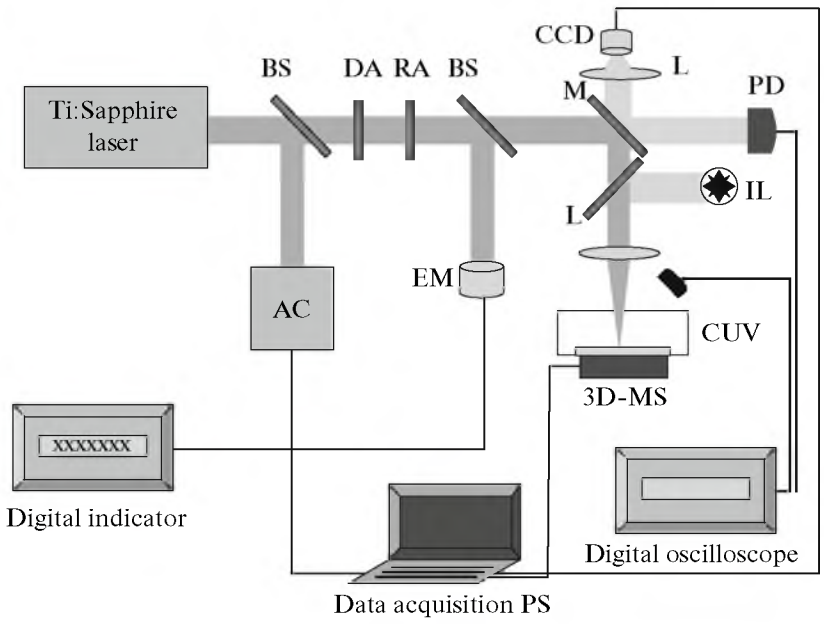

Fig. 1. The scheme of an experimental setup for the nano and micro structuring of surfaces. (BS) semitransparent mirror, (DA, RA) diffraction and reflection attenuators, (AC) autocorrelator, (PD) photodiode, (EM) thermoelectric energy meter, (M) mirror, (L) quartz lens, (CCD) video camera, (IL) illumination lamp, (CUV) glass cuvette with a specimen, and (3D-MS) 3D-moving support with a motor.

on a spot 1 mm in diameter (at the level $1/e^2$) with normal incidence onto a fixed aluminum target and one moving at a velocity of 60 μm/s, respectively. The target was placed in a plastic bath into which water was poured in some experiments to create a thin (1–1.5 mm) water layer.

To study the optical characteristics of photoexcited aluminum on the fresh spots of the material surface, we measured factors of self-reflection at an angle of 45° of the isolated focused linearly polarized femtosecond laser pulses at the wavelength $\lambda \approx 800$ nm depending on the fluence of the absorbed energy. The energy of the mirror-reflected radiation was measured using the pyroelectric detector at different values of the incident energy of isolated pulses.

RESULTS

When the aluminum specimen is exposed in air to the IR femtosecond laser radiation at the wavelength $\lambda \approx 744$ nm with the fluence $F = 0.22$ J/cm^2 and the number of pulses $N = 60$, the formation of the one-dimensional surface periodic subwave grating (Fig. 2) is observed with the mean period $\Lambda \approx 0.53$ μm. The resulting structures have a relatively clearly identified directivity across the polarization vector of the incident electromagnetic radiation, which is the main evidence for the interferential nature of these structures [10]. When the fluence decreases from 0.17 to 0.09 J/cm^2 within the range of numbers of incident laser pulses from $N = 1000$ to $N = 3000$, the pronounced one-dimensional periodic structures are not observed, although degraded quasiperiodic structures with the period $\Lambda \approx 0.5$ μm are noticeable in some areas. It should be noted that all surface structures in air are obtained at fluences substantially smaller than the ablation threshold of the bulk aluminum $F_{abl} = 0.74$ J/cm^2 [11].

A somewhat different situation occurs when the specimen subject to the IR femtosecond laser structuring is covered with a millimeter-thick layer of water. In this case the periodic modulation of the relief during the multipulse ($N = 300$–3000) regime of imprinting was already observed at an fluence slightly larger than 0.06 J/cm^2. Figure 3 presents the evolution of the surface topology with the N growth and, as can be seen, the more laser pulses there are incident on the surface, the more pronounced the Fourier component of the surface's spatial spectrum becomes; this corresponds to the mean period of the surface grating $\Lambda \approx 0.43$ μm. The width of the nanohills proper was about 60 nm.

Using UV femtosecond laser radiation with the wavelength $\lambda = 248$ nm, an fluence reaching 0.06 J/cm^2, and $N = 60$ pulses did not yield the creation of one-dimensional surface nanogratings. As can be seen in Fig. 4, in this case the periodic modulation of the surface with the mean period $\Lambda \approx 0.18$ μm occurs only locally in areas less than 1 μm^2. Such a pattern is similar to the structuring of the dry aluminum surface by IR pulses with fluences below the threshold of the periodic nanorelief formation.

It is also important to note that all surface spots processed by IR and UV femtosecond laser pulses

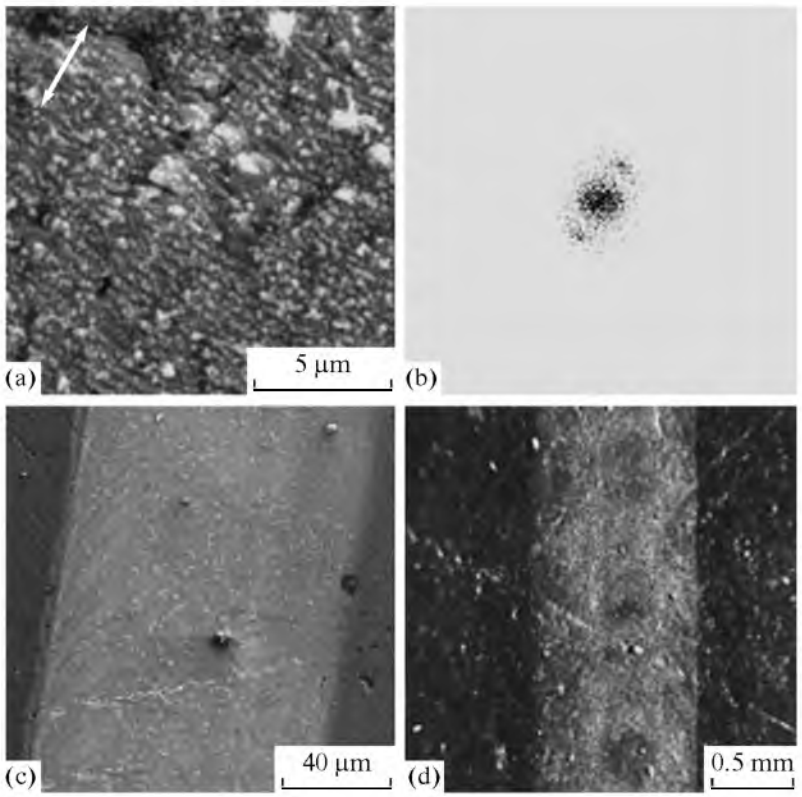

Fig. 2. (a) An SEM image of the structured aluminum surface with the fluence $F = 0.22$ J/cm^2 and number of interacted pulses $N = 60$ (the arrow indicates the direction of incident radiation). (b) The two-dimensional Fourier transform of the surface. (c) The general view of the structured area obtained using SEM. (d) The same obtained using an optical microscope.

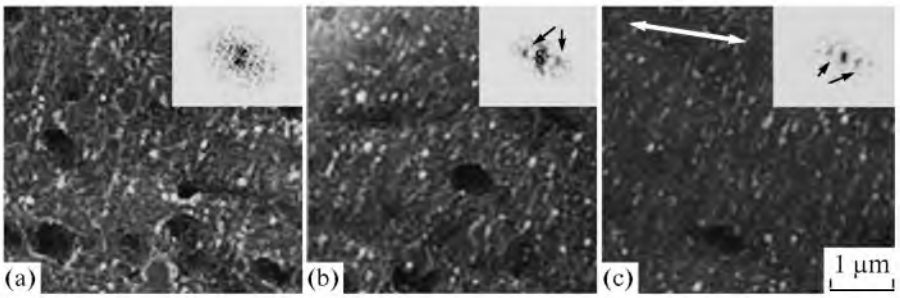

Fig. 3. SEM images of aluminum surfaces struturized under the water layer with the fluence of laser pulse $F = 0.13$ J/cm^2 and with different numbers of pulses: (a) 300, (b) 1000, and (c) 3000. The two-dimensional Fourier spectrum of the respective surface is depicted at the corner of each image.

acquired a yellowish color and the size of the nanostructurized area observed in the SEM coincides exactly with the changed-color area of the material surface (see Fig. 2); moreover, as both the number of structurizing laser pulses and fluence increased, the surface color became more and more pronounced, which was related to the growth in density of nanostructures per unit surface area (Fig. 5). The reason for the change in color of the aluminum surface is supposedly associated with the plasmonic resonance shift to the near-UV region so that part of the absorption peak is located in the blue region of the visible range [9].

RESULTS AND DISCUSSION

An analysis of SEM images showed that flocculent submicro and nanoformations are mainly formed on samples with dry surfaces at small fluences $F_{col} < F < 0.17$ J/cm^2 and at a laser-radiation wavelength of $\lambda = 744$ nm, where $F_{col} = 0.045$ J/cm^2 is the value of the threshold of modification (coloring) of the dry surface for the isolated pulse (Fig. 6). Periodic nanostructures were imprinted on the dry surface only when fluences were larger than $F_{nano} = 0.19 \pm 0.02$ J/cm^2; moreover,

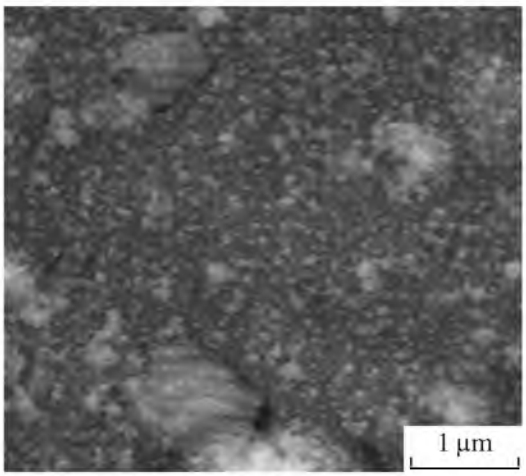

Fig. 4. SEM image of the surface nanoroughness with the local occurrence of periodic structures. Fluence $F = 0.12$ J/cm^2, number of pulses $N = 30$, and laser wavelength $\lambda = 248$ nm.

the larger the fluence is, the smaller the number of pulses are needed to make the surface relief periodic.

The nanostructures imprinted under the water layer differ qualitatively from those obtained on the dry surface. In the first place, we observed in experiments under the water layer that flocculent formations are almost completely absent, which was also observed in [9] where the structuring was conducted using ethanol. In the second place, the threshold values F_{col} of the formation of nonregular surface nanostructures were distinct—the threshold in water ($F_{col} = 0.03$ J/cm^2) was 1.5 times lower than in air (see Fig. 6)—and the formation of a periodic nanorelief in air requires about three times the fluence F_{nano} in water.

Similar structures were obtained in other works [8, 9]; however, one-dimensional periodic modulation was not observed in [9] and the periodicity in [8] was achieved at considerably smaller energy fluencies, which may be associated with the difference in the laser-radiation wavelengths used, because, near 800 nm (the photon energy is 1.5 eV), a substantial contribution to aluminum permittivity takes place from the interband transitions [12].

CALCULATION OF PERIODS OF SURFACE NANOGRATINGS

Values of surface nanograting periods for $\lambda = 744$ nm may be estimated using the interferential model and optical characteristics of photoexcited aluminum, namely, the electron-temperature relationship of the electron-gas permittivity described by the Drude model. It follows from the interferential model that the occurrence of a laser-induced surface periodic structure is connected with the interference of an incident electromagnetic wave with the surface plasmon excited by the wave; the period of such a structure (Λ) is equal to the plasmon wavelength. The disperse relationship for surface plasmons that propagate along the flat surface of the metal bordering dielectric appears as [13]

$$k_{sp} = \frac{\omega}{c}\sqrt{\frac{\varepsilon_m \varepsilon_d}{\varepsilon_m + \varepsilon_d}}, \qquad (1)$$

where k_{sp} is the (complex-valued) wavevector of a surface plasmon, ω is the frequency of the exciting electromagnetic wave, c is the light speed in vacuum, and $\varepsilon_m = \varepsilon_1 + i\varepsilon_2$ and ε_d are the complex permittivities of the metal and the dielectric adjacent to the surface. Any decay in dielectric can be neglected to a high accuracy, but there is an extreme need to take into account the permittivity's imaginary part for aluminum in the frequency range of the near-IR region ($\hbar\omega \sim 1.6$ eV). Then, from Eq. (1), with regard for an imaginary part of aluminum permittivity and from the relation between a real part of the wavevector of the surface plasmon and its period, we can derive

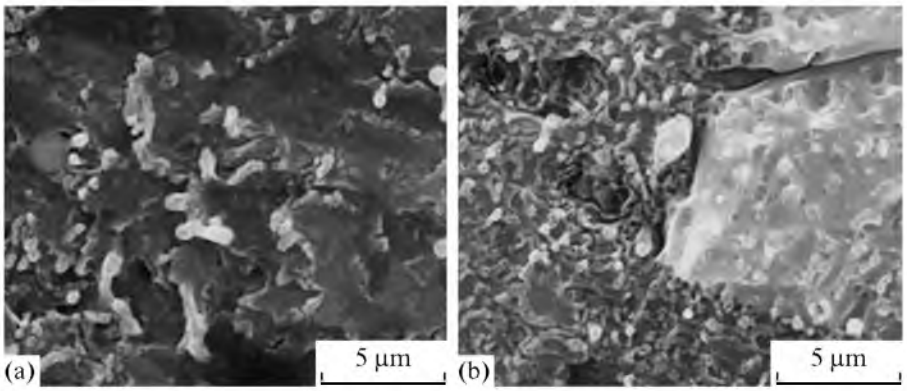

Fig. 5. The aluminum surface structures obtained under the water layer with the identical number of pulses $N = 300$ and different fluences: (a) $F = 45$ mJ/cm^2 and (b) $F = 130$ mJ/cm^2. The number of nanostructures per unit surface-area grows as the fluence increases.

$$\mathrm{Re}(k_{sp}) = \frac{2\pi}{\Lambda} \cong \frac{\omega}{c}\sqrt{\frac{\varepsilon_d[\varepsilon_1(\varepsilon_d+\varepsilon_1)+\varepsilon_2^2]}{(\varepsilon_d+\varepsilon_1)^2+\varepsilon_2^2}}. \qquad (2)$$

There is a certain difficulty in choosing the permittivity of a dielectric which is connected with the presence of the natural oxide layer of aluminum. We can take it into account by two methods, either by considering the laminated structure of the metal–oxide–atmosphere or by completely neglecting the atmosphere (for the single purpose of estimating the surface-structure period) and considering the surface plasmon propagation only along the metal–oxide border. In order to interpret the experimental data, for simplicity we used a second, more rough, assumption (ε_d(744 nm) = 3.17) which, with regard for an additional laser-induced oxidation of the aluminum surface under the multipulse laser action, nevertheless, yielded values of nanograting periods close to the experimental results and allowed us to explain the reason for this small difference in period values for imprinting the surface nanogratings in various media.

For the interaction between femtosecond laser pulses and metals, it is necessary to consider the surface heating process as the instantaneous heating of conduction electrons to temperatures on the order of several electron volts while the grating's temperature remains close to the initial value. The electron-relaxation time (on the order of the pulse duration) is mainly determined by electron–electron collisions; then, from the Drude model with consideration for the grating's contribution $\varepsilon_b(\omega)$, we have [14]

$$\varepsilon_m(\omega) = \varepsilon_b(\omega) - \frac{\omega_p^2}{\omega^2+\gamma_{ee}^2}\left(1 - i\frac{\gamma_{ee}}{\omega}\right), \qquad (3)$$

where ω_p is the plasma frequency ($\hbar\omega_p$ = 12.7 eV for aluminum [15]); ε_b(744 nm) $\cong -10.8 + i38.7$ is the lattice contribution to aluminum permittivity, which is found by subtracting from the total aluminum permittivity [15] the calculated Drude contribution of conduction electrons with the parameters $\omega = 2.53 \times 10^{15}$ s^{-1}, $\omega_p = 1.93 \times 10^{16}$ s^{-1} and from Eq. (4) τ_{ee}(300 K) = 1.87×10^{-14} s; $\gamma_{ee} = \dfrac{1}{\tau_{ee}(T_e)}$ is the inverse time of electron collisions, which is determined by the known [16] expression

$$\tau_{ee}(T_e) = K_{ee}^{-1}\frac{1+\exp[(E_F-E)/k_B T_e]}{(\pi k_B T_e)^2+(E_F-E)^2}; \qquad (4)$$

$K_{ee} = \dfrac{\pi^2\sqrt{3}\omega_p}{128E_F^2}$ (K_{ee} = 0.0192 fs^{-1} eV^{-2} for aluminum); E_F is the Fermi energy (E_F = 11.7 eV for aluminum); k_B is the Boltzmann constant; and E is the energy of the excited conduction electrons, which actually is equal to $E_F + \hbar\omega$. Substituting the obtained values of the function $\gamma_{ee}(T_e)$ in Eq. (3), we derive the electron-temperature dependences of the real and imaginary parts of permittivity. A similar calculation for femtosecond laser pulses at other wavelengths for aluminum was performed in [17, 18]. The resulting functions $\gamma_{ee}(T_e)$, $\mathrm{Re}\varepsilon_m(T_e)$, and $\mathrm{Im}\varepsilon_m(T_e)$ for λ = 744 nm (Fig. 7) demonstrate how substantial the influence of laser excitation and electron temperature is, particularly on the optical characteristics of aluminum.

The dependence that the temperature of nonequilibrium electron gas (T_e) has on the fluence of the inci-

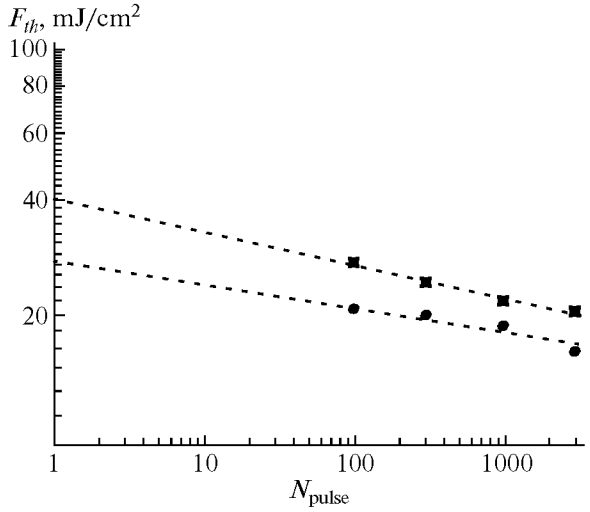

Fig. 6. Experimental dependences that the threshold of the aluminum surface coloring has on the number of laser pulses. The squares show the structuring of the dry surface ($F_{col}(1)$ = 0.045 J/cm^2); circles show the surface under the water layer ($F_{col}(1)$ = 0.03 J/cm^2).

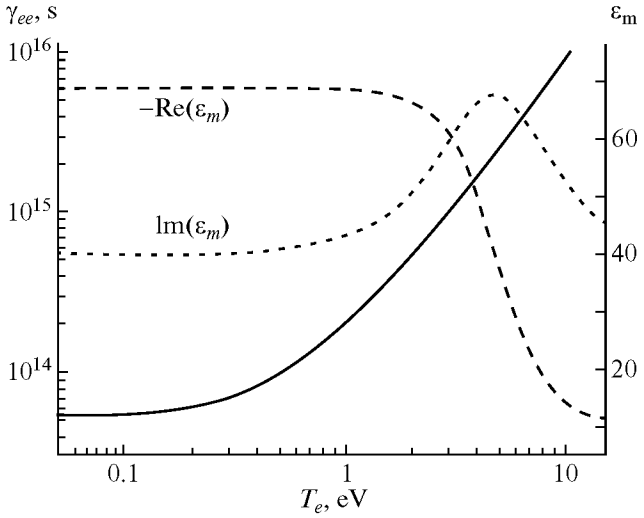

Fig. 7. Dependences that the electron-collision rate (solid line, left axis) and the real (dashed line, right axis, with the sign inversed) and imaginary (dotted line, right axis) parts of the aluminum permittivity have on the electron temperature for λ = 744 nm.

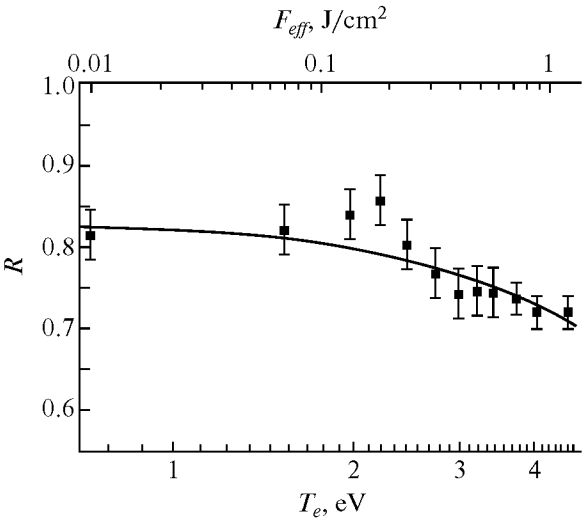

Fig. 8. Comparison between experimental data (depending on the fluence, which is indicated by squares) and theoretical values (as a function of the electron temperature, shown as a solid line) of the self-reflection factor for the incidence angle $\theta = 45°$ of the *p*-polarized femtosecond laser pulse ($\lambda = 800$ nm).

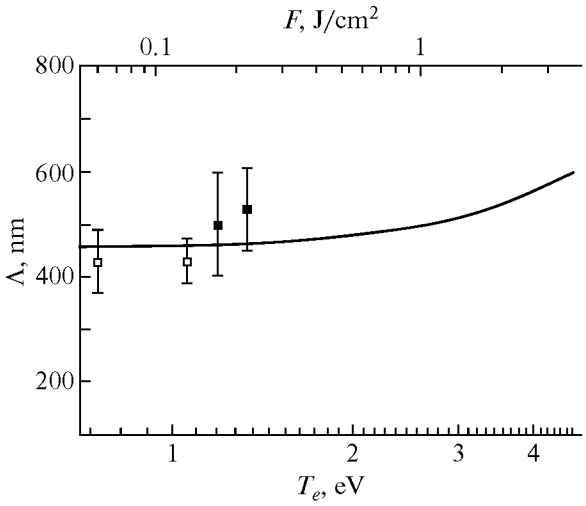

Fig. 9. Comparison between experimental data and the results of a calculation of the period of surface nanogratings for the wavelength of the femtosecond laser radiation $\lambda = 744$ nm. Black squares are values relating to structuring in air; empty circles are those in water.

dent femtosecond laser radiation may be estimated as follows. Having found the instantaneous optical characteristic of the aluminum surface, we can calculate the self-reflection of the pumping pulse depending on the electron temperature from Fresnel formulas and compare these values to the experimental data on the self-reflection of pumping pulses. Figure 8 presents a comparison of the calculational dependence of the self-reflection factor R of the IR femtosecond laser pulse for the incidence angle $\theta = 45°$ to experimental data for the same conditions.

The thus-compared calculational and experimental values in the logarithmic abscissa axes give the direct relation between the absorbed fluence (F_{eff}) of laser radiation and the electron temperature. The absorbed fluence is expressed through the incident fluence as

$$F_{\text{eff}} = F[1 - R(F_{\text{eff}})], \qquad (5)$$

where $R(F_{\text{eff}})$ is the factor of reflection from the surface, which is also a function of the electron temperature and is calculated from the Fresnel formulas.

Having calculated the period of the surface plasmon from Eq. (2) with consideration for the electron-temperature dependence of permittivity (Eqs. (3) and (4)), we derive the dependence that the nanograting period has on the temperature of electron gas because it follows from the interferential model that the surface-nanograting period coincides with the surface-plasmon period. Further, using the derived dependence that the electron temperature has on the fluence of laser energy incident on the aluminum surface, we can construct the dependence that the surface-nanograting period has on the fluence. A comparison of the theoretical and experimental values of the period of the surface nanogratings on aluminum is shown in Fig. 9, from which it is clear that the experimental and calculational values of a period of the surface one-dimensional nanograting increase as the fluence of laser radiation grows.

CONCLUSIONS

Thus, using electronic and optical microscopy, in this work we investigated periodic and nonperiodic nanostructures on the aluminum surface which were obtained at two wavelengths (744 and 248 nm) of femtosecond laser radiation in a wide range of numbers of pulses ($N = 10$–3000) both on a dry surface and under the water layer. It was revealed that the period of the one-dimensional periodic nanograting depends on the wavelength; i.e., $\Lambda = 430$–530 nm for $\lambda = 744$ nm, $\Lambda \approx 180$ nm for $\lambda = 248$ nm, and the orientation of ripples is perpendicular to the polarization of the incident electromagnetic wave, which corresponds to the conclusions from the interferential model.

Nanostructures obtained using IR femtosecond laser radiation are of the most interest because their period is substantially less than that of earlier-obtained structures in [8] and, unlike structuring by radiation in the UV region, the periodicity of the surface relief is observed on a significant area of the laser spot rather than locally on small spots of the surface.

A comparison between the electron temperature and the surface fluence of the incident laser radiation allowed us to theoretically estimate the values of the surface-nanograting periods depending on the latter factor. The theoretical values of the nanograting-surface periods obtained from the onterferential model

with consideration for the influence that the electron–electron relaxation time has on optical characteristics are in a good agreement with our experimental data.

The thresholds of modification of the optical characteristics were also estimated for air (0.045 J/cm^2) and water (0.03 J cm^2); i.e., the conditions for creating the so-called golden aluminum, whose color is permanent and independent of the quality of the surface polish, were determined.

REFERENCES

1. F. J. Garcia-Vidal and J. B. Pendry, Phys. Rev. Lett. **77**, 1163 (1996).
2. C. K. Chen, A. R. B. de Castro, and Y. R. Shen, Phys. Rev. Lett. **46**, 145 (1981).
3. M. Birnbaum, J. Appl. Phys. **36**, 3688 (1965).
4. E. V. Golosov, L. I. Emel'yanov, A. A. Ionin, Yu. R. Kolobov, S. I. Kudryashov, A. E. Ligachev, Yu. N. Novoselov, L. V. Seleznev, and D. V. Sinitsyn, Pis'ma Zh. Eksp. Teor. Fiz. **90** (2), 116 (2009) [JETP Lett. **90** (2), 107 (2009)].
5. J. Wang and C. Guo, Appl. Phys. Lett. **87**, 251914 (2005).
6. S. I. Kudryashov, E. V. Golosov, A. A. Ionin, Yu. R. Kolobov, A. E. Ligachev, S. V. Makarov, Yu. N. Novoselov, L. V. Seleznev, and D. V. Sinitsyn, Proc. SPIE—Int. Soc. Opt. Eng. **7719**, 771921 (2010).
7. J. Bonse, A. Rosenfeld, and J. Kruger, J. Appl. Phys. **106**, 104910 (2009).
8. A. Y. Vorobyev and C. Guo, Appl. Phys. Lett. **92**, 041914 (2008).
9. E. Stratakis, V. Zorba, M. Barberoglou, C. Fotakis, and G. A. Shafeev, Nanotechnology **20**, 105303 (2009).
10. J. E. Sipe, J. F. Young, J. S. Preston, and H. M. van Driel, Phys. Rev. B: Condens. Matter **27** (2), 1141 (1983).
11. S. I. Anisimov and N. A. Inogamov, Appl Phys A: Mater. Sci. Process. **92**, 939 (2008).
12. H. Ehrenreich, H. R. Philipp, and B. Segall, Phys. Rev. **132** (5), 1918 (1963).
13. V. V. Klimov, *Nanoplasmonics* (Fizmatlit, Moscow, 2010; Pan Stanford, Singapore, 2011).
14. N. Del Fatti, R. Bouffanai, F. Vallee, and C. Flytzanis, Phys. Rev. Lett. **81**, 922 (1998).
15. *Handbook of Optical Constants of Solids*, Ed. by E. D. Palik (Academic, New York, 1998).
16. R. Groeneveld, R. Sprik, and A. Lagendijk, Phys. Rev. B: Condens. Matter **51** (17) 11433 (1995).
17. M. B. Agranat, N. E. Andreev, S. I. Ashitkov, M. E. Veshman, P. R. Levashov, A. V. Ovchinnikov, D. S. Sitnikov, V. E. Fortov, and K. V. Khishchenko, Pis'ma Zh. Eksp. Teor. Fiz. **85** (6), 328 (2007) [JETP Lett. **85** (6), 271 (2007)].
18. N. A. Inogamov, V. V. Zhakhovskii, S. I. Ashitkov, V. A. Khokhlov, Yu. V. Petrov, P. S. Komarov, M. B. Agranat, S. I. Anisimov, and K. Nishihara, Appl. Surf. Sci. **255**, 9712 (2009).